Probability-Density-Dependent Load Frequency Control of Power Systems With Random Delays and Cyber-Attacks via Circuital Implementation

Shen Yan, Zhou Gu, *Member, IEEE*, Ju H. Park, *Senior Member, IEEE*, Xiangpeng Xie, *Member, IEEE*, and Chunxia Dou, *Senior Member, IEEE*

***Abstract*—This paper studies the decentralized H_∞ secure load frequency control issue and circuital realization of multi-area networked power systems subject to random transmission delays and deception attacks. To make full use of the stochastic feature of the network-induced transmission delay, its distribution described by the probability density function is utilized. Due to this feature, the normal control signal and the injected deceptive attack signal transmitted over the network can be formed as two distributed delay terms. Then, the *i*th load frequency control area is established as a new distributed delay system, in which the delay probability density is treated as the distributed kernel. By utilizing an integral inequality dependent on the kernel, new sufficient controller design conditions are derived to guarantee the system stability with given H_∞ performance. Moreover, a physical execution approach is addressed to transfer the load frequency control systems into electrical analogy circuits. The effectiveness of the proposed approach is illustrated via the professional simcape toolbox in Simulink/MATLAB for circuit simulations.**

***Index Terms*—Networked power systems, random transmission delays, cyber attacks, load frequency control, circuital implementation.**

Manuscript received 28 January 2022; revised 8 April 2022; accepted 24 May 2022. Date of publication 30 May 2022; date of current version 21 October 2022. This work was supported in part by the National Natural Science Foundation of China under Grant 62103193 and Grant 62022044; in part by the Natural Science Foundation of Jiangsu Province of China under Grant BK20200769; in part by the Natural Science Foundation of Jiangsu Provincial Universities under Grant 20KJB510045; in part by the Project funded by China Postdoctoral Science Foundation under Grant 2021TQ0155; in part by the Jiangsu Natural Science Foundation for Distinguished Young Scholars under Grant BK20190039. The work of Ju H. Park was supported by the National Research Foundation of Korea (NRF) grant funded by the Korea Government (MSIT) under Grant 2020R1A2B5B02002002. Paper no. TSG-00141-2022. *(Corresponding authors: Zhou Gu; Ju H. Park.)*

Shen Yan and Zhou Gu are with the College of Mechanical and Electronic Engineering, Nanjing Forestry University, Nanjing 210037, China (e-mail: yanshenzdh@gmail.com; gzh1808@163.com).

Ju H. Park is with the Department of Electrical Engineering, Yeungnam University, Gyeongsan 38541, South Korea (e-mail: jessie@ynu.ac.kr).

Xiangpeng Xie is with the Institute of Advanced Technology, Nanjing University of Posts and Telecommunications, Nanjing 210023, China, and also with the School of Information Science and Engineering, Chengdu University, Chengdu 610106, China (e-mail: xiexp@njupt.edu.cn).

Chunxia Dou is with the Institute of Advanced Technology for Carbon Neutrality, Nanjing University of Posts and Telecommunications, Nanjing 210023, China (e-mail: cxdou@ysu.edu.cn).

Color versions of one or more figures in this article are available at https://doi.org/10.1109/TSG.2022.3178976.

Digital Object Identifier 10.1109/TSG.2022.3178976

I. Introduction

AS WE known, there are basically three layers of the control framework of power systems, which are primary control (conventional droop control), secondary control (voltage/frequency regulation), and tertiary control (economic dispatch and power flow optimization) [1]. As a representative secondary control, load frequency control (LFC) is a critical strategy to maintain the frequency stable for power systems and much effort has been devoted to studying it [2]–[8]. In a multi-area power system, the centralized strategy of LFC utilizing global system information and the distributed control method using the neighbor subsystem information are effective strategies to regulate the system frequency. Nevertheless, the utilization of power interchange through tie-lines among subsystems increases the complexity and difficultly of frequency regulation. Compared with them, the decentralized LFC scheme investigated in [9], [10] is more practical and easier for implementation because only the local area information is utilized to attenuate the frequency deviation. In recent years, as the trend of the integration of physical power systems and communication network, networked power systems (NPSs) have received much attention from a lot of researchers.

With the introduction of communication network, the network-induced delay is a common phenomenon, which could degrade the system performance, even make system unstable [11]. However, some published results of LFC systems using proportional-integral (PI) controller have not considered the network communication delay [12]. To tackle this problem, a decentralized LFC method for power systems with multi constant communication delays is developed in [13], where the constant delays are treated as multiplicative uncertainties. Reference [14] addresses a new decentralized sliding mode LFC scheme for multi-area NPSs with constant delay and wind power integration. Since the situation of communication network is usually uncertain and varying, a time-varying delay model is more practical than the constant one. Due to this fact, some delay-dependent controller design conditions are derived for LFC systems with time-varying communication delays [15]. In [16], a power system model with multiple time-varying communication delays is established and delay-dependent conditions for designing H_∞ controller are obtained. Most of the existing outcomes, for

instance [15], [16], are accomplished based on the interval time-varying delay method and boundary information of the communication delay. It is worthy noting that the time-varying communication delays in [15], [16] are assumed to be with a uniform distribution. Practically, for a real TCP/IP-based communication network, communication delay often has stochastic properties. Generally speaking, it is usually distributed with some probabilistic features [17]–[19]. Thus, the uniform distribution assumption without using these features may yield conservative results. Considering the inter features of the communication delay in system analysis/synthesis, less conservative conditions are expected to be obtained. As a fact, the probability density is more specific and precise for depicting the random delay.

On the other hand, the security of communication network that is vulnerable to be wrecked by hackers is very important for NPSs. If the remote control signals transmitted over the network are injected by some false data, the NPS will be difficult to be maintained at the nominal state. Over the past decade, much attention has been paid to the control problem against cyber-attacks, such as Denial-of-service (DoS) attack [21], [22], deception attack [23], [24]. Concretely speaking, a resilient event-triggered LFC approach for NPSs subject to DoS attack with finite energy is addressed in [20]. Different from DoS attack by blocking the connections of nets, deception attack aims to change the real value of control signal by injecting a false data, which makes it more deceptive. Considering multi-area NPSs with time-varying communication delay and deception attack, a resilient LFC approach is addressed in [25], in which the deception attack is described as a time-varying delay-dependent function. Reference [26] studies the H_∞ LFC issue of multi-area NPSs with DoS attack and deception attack, which is also modeled as a time-varying delay-dependent function. In [25], [26], the time-varying delay-dependent deception attack model is established only by using the bounds of delays. Compared to the conventional interval time-varying delay method, using not only the upper and lower bounds, but also the delay probability distribution is potential for obtaining less conservative results.

It is known that testing the effectiveness of control strategies in some practical systems is costly and difficult. Therefore, it is worthy to develop suitable hardware simulators for some real control systems. Due the fact that many control devices of practical systems are executed by electrical equipments, it is natural and reasonable to transform the physical systems into analogy circuits to verify the validity of control method and save the testing cost. For instance, a circuital implementation method is studied to convert the robust adaptive fault tolerant control schemes into electrical circuits in [27]. For uncertain nonlinear multi-agent systems with actuator faults, the adaptive control issue is developed and its circuital realization is studied in [28].

Based on the above motivations, this article addresses the H_∞ load frequency regulation of NPSs with random delays and cyber-attacks in a decentralized method. A circuital realization approach is proposed to simulate the dynamics of power system components and the controller via equivalent analogy circuits. The following new challenging problems are introduced in developing the model and obtaining the stability and synthesis conditions.

1) Since the existing methods [15], [25], [26] based on an interval time-varying delay model do not take into account the probability distribution of random delay, how to model the random delay by making use of the distribution information is the first challenging problem.

2) Considering the first challenging problem, a new distributed delay model with the kernel representing the delay distribution will be proposed in this paper. However, the existing method [29] based on Legendre polynomials to handle this new model will cause approximation error and further lead to conservative results. Thus, how to remove such approximation error and reduce conservativeness is the second challenging problem.

3) There exist stochastic transmission delays when the attackers inject attack signals into network, therefore, how to model and deal with the deception attack will also bring the challenging problem similar with handling the random delay.

To solve these challenging issues, the main contributions of this work are given below:

1) To make efficient use of the stochastic feature of the network-induced transmission delay, a novel distributed delay model with kernel is established, where the kernel is used to represent the delay probability density. To model the random deception attacks, not only the stochastic feature induced by attacker, but also the stochastic feature caused by random delays are considered in this paper. Then, a new representation of random delay and deception attack is proposed for the first time. This model is more general than the traditional one based on interval time-varying delay method [15], [25], [26].

2) In the existing result [29], the distributed delay with kernel is approximated by Legendre polynomials and handled by Bessel-Legendre inequality, which could lead to approximation error and design conservativeness. To solve this problem, the distributed kernel is utilized directly to construct a new Lyapunov-Krasovskii functional (LKF) in this paper. An integral inequality based on the kernel is used to deal with the distributed delay term directly without any approximation error. Then, new sufficient and less conservative conditions formed by linear matrix inequalities (LMIs) are derived to design the decentralized H_∞ secure controller.

The organization of this paper is provided as follows. The preliminaries of modeling the closed-loop NPS is given in Section II. Then the stability and controller design conditions are obtained in Section III. Some simulation results are implemented in Section IV. Section V summaries the conclusions and presents some future investigations.

Notation: In this paper, we define $\mathbf{He}(A) = A + A^{\mathsf{T}}$. $\otimes$ means the Kronecker product. $\mathbf{Sy}(A, B) \triangleq B^{\mathsf{T}}AB$. $\binom{a}{b}$ denotes $\frac{a!}{(a-b)!b!}$.

II. Preliminaries

In the LFC problem of power systems, there exist some complicate nonlinear dynamics. Due to the fact that the load

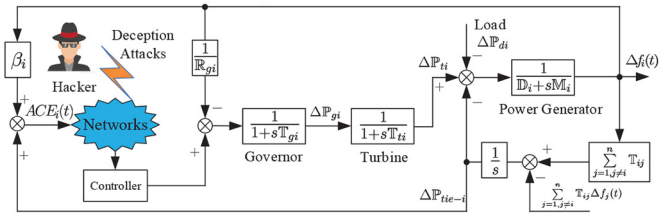

Fig. 1. The ith control area of a multi-area LFC NPS.

variations of power system are usually small, it is permissible and useful to linearize them around the operating point [30], [31]. In many existing results [6]–[8], [31], the dynamics of governor, turbine and power generator are linearized as the following first-order transfer functions:

$$\begin{cases} \text{Governor}: & G_{gi}(s)=\frac{1}{1+s\mathbb{T}_{gi}}, \\ \text{Turbine}: & G_{ti}(s)=\frac{1}{1+s\mathbb{T}_{ti}}, \\ \text{Power generator}: & G_{pi}(s)=\frac{1}{\mathbb{D}_i+s\mathbb{M}_i}. \end{cases}$$

where $\mathbb{T}_{gi}$, $\mathbb{T}_{ti}$, $\mathbb{D}_i$, $\mathbb{M}_i$ and $\mathbb{R}_{gi}$ are the governor and turbine time constants, damping coefficient, inertia moment of generator and droop coefficient of the ith control area, respectively.

In this paper, following the above linearization method, the structure of the linear dynamic model of the ith control area in a multi-area NPS is illustrated in Fig. 1. Let $\Delta f_i(t)$, $\Delta\mathbb{P}_{tie-i}(t)$, $\Delta\mathbb{P}_{gi}(t)$, $\Delta\mathbb{P}_{ti}(t)$ and $\Delta\mathbb{P}_{di}(t)$ represent the deviations of system frequency, tie-line power exchange, valve position, mechanical output of turbine and load disturbance of the ith control area, respectively. Then, the differential equations to describe the system dynamics of the ith control area [6], [25] are given as:

$$\begin{cases} \Delta\dot{f}_i(t)=\frac{1}{\mathbb{M}_i}(\Delta\mathbb{P}_{ti}(t)-\Delta\mathbb{P}_{di}(t) \\ \quad -\Delta\mathbb{P}_{tie-i}(t)-\mathbb{D}_i\Delta f_i(t)) \\ \Delta\dot{\mathbb{P}}_{tie-i}(t)=\sum_{j=1,j\neq i}^{n}\mathbb{T}_{ij}\big(\Delta f_i(t)-\Delta f_j(t)\big) \\ \Delta\dot{\mathbb{P}}_{gi}(t)=\frac{1}{\mathbb{T}_{gi}}\Big(u_i(t)-\frac{1}{\mathbb{R}_{gi}}\Delta f_i(t)-\Delta\mathbb{P}_{gi}(t)\Big) \\ \Delta\dot{\mathbb{P}}_{ti}(t)=\frac{1}{\mathbb{T}_{ti}}\big(\Delta\mathbb{P}_{gi}(t)-\Delta\mathbb{P}_{ti}(t)\big) \end{cases}. \tag{1}$$

The ith area control error signal used to maintain zero steady-state error for frequency deviation is defined as

$$ACE_i(t)=\beta_i\Delta f_i(t)+\Delta\mathbb{P}_{tie-i}(t), \tag{2}$$

where β_i denotes the frequency bias factor.

Selecting the same state, output and disturbance in [25] as $x_i^{\mathsf{T}}(t) = [\Delta f_i(t), \Delta\mathbb{P}_{tie-i}(t), \Delta\mathbb{P}_{gi}(t), \Delta\mathbb{P}_{ti}(t), \int ACE_i(t)dt]^{\mathsf{T}}$, $y_i(t)=[ACE_i(t) \ \ \int ACE_i(t)dt]^{\mathsf{T}}$ and $\omega_i(t)=[\Delta\mathbb{P}_{di}(t) \ \ \varpi_i(t)]^{\mathsf{T}}$ ($\varpi_i(t)\triangleq\sum_{j=1,j\neq i}^{n}\mathbb{T}_{ij}\Delta f_j(t)$), one can represent the ith LFC system in the form of state-space by:

$$\begin{cases} \dot{x}_i(t)=\mathcal{A}_ix_i(t)+\mathcal{F}_i\omega_i(t)+\mathcal{B}_iu_i(t) \\ y_i(t)=\mathcal{C}_ix_i(t) \\ z_i(t)=\mathcal{C}_ix_i(t) \end{cases}, \tag{3}$$

in which $z_i(t)$ is the performance output and

$$\mathcal{A}_i=\begin{bmatrix} -\frac{\mathbb{D}_i}{\mathbb{M}_i} & -\frac{1}{\mathbb{M}_i} & 0 & \frac{1}{\mathbb{M}_i} & 0 \\ \sum_{j=1,j\neq i}^{n}\mathbb{T}_{ij} & 0 & 0 & 0 & 0 \\ -\frac{1}{\mathbb{R}_{gi}\mathbb{T}_{gi}} & 0 & -\frac{1}{\mathbb{T}_{gi}} & 0 & 0 \\ 0 & 0 & \frac{1}{\mathbb{T}_{ti}} & -\frac{1}{\mathbb{T}_{ti}} & 0 \\ \beta_i & 1 & 0 & 0 & 0 \end{bmatrix}, \mathcal{B}_i=\begin{bmatrix} 0 \\ 0 \\ \frac{1}{\mathbb{T}_{gi}} \\ 0 \\ 0 \end{bmatrix},$$

$$\mathcal{C}_i=\begin{bmatrix} \beta_i & 1 & 0 & 0 & 0 \\ 0 & 0 & 0 & 0 & 1 \end{bmatrix}, \mathcal{F}_i^{\mathsf{T}}=\begin{bmatrix} -\frac{1}{\mathbb{M}_i} & 0 & 0 & 0 & 0 \\ 0 & -1 & 0 & 0 & 0 \end{bmatrix}.$$

In order to keep the frequency $\Delta f_i(t)$ at the prescribed value, the following decentralized LFC scheme based on the conventional PI control is utilized:

$$u_i(t)=\mathcal{K}_{Pi}ACE_i(t)+\mathcal{K}_{Ii}\int ACE_i(t)dt=\mathcal{K}_iy_i(t), \tag{4}$$

where $\mathcal{K}_i=[\mathcal{K}_{Pi} \ \ \mathcal{K}_{Ii}]$ and $\mathcal{K}_{Pi}$, $\mathcal{K}_{Ii}$ are the PI controller gains to be designed.

When the control signal is transmitted over the communication network, it is highly possible that the transmitted signal is delayed and damaged by sudden congestion and malicious attackers. Considering these factors, the output of controller with delay and deception attack is represented as

$$u_i^a(t)=\mathcal{K}_i\mathcal{C}_ix_i(t-\tau(t))+\lambda(t)\mathcal{K}_i\varphi_i(t-\tau(t)), \tag{5}$$

where $\tau(t)\in[0,h]$ means the random transmission delay; h is the upper bound of the delay; $\lambda(t)\in\{0, \ 1\}$ is a Bernoulli variable to describe the occurrence of deception attack by $\lambda(t)=1$ and no attack $\lambda(t)=0$; the mathematical expectations of $\lambda(t)=1$ and $\lambda(t)=0$ are $\mathbb{E}\{\lambda(t)=1\}=\bar{\lambda}$ and $\mathbb{E}\{\lambda(t)=0\}=1-\bar{\lambda}$, respectively.

In some existing results [8], [26], the deception attack is usually bounded and modeled by a Lipschitz nonlinear function related with system state or output. Following the same way in [8], [26], the deception signal $\varphi_i(t)$ is assumed to satisfy

$$\|\varphi_i(t)\|_2\leq\|\mathcal{H}_i\mathcal{C}_ix_i(t)\|_2, \tag{6}$$

where $\mathcal{H}_i$ is a given constant matrix used to describe the upper bound of deception attack.

It is noted that the random transmission delay $\tau(t)$ usually meets some probability distributions. For convenience, we abbreviate $\tau(t)$ as τ. For example, based on the described scenarios in [18], [32] to simulate the network channel, the communication delay with upper bound $h=0.2s$ and its normalized distribution histogram are drawn in Fig. 2.

To utilize the random information of delay τ, its probability density described by the kernel $g(\cdot)$ with $\int_0^h g(s)ds=1$ is considered, which can be accessible by statistical method. In Fig. 2, a probability density function $g(\tau)$ is used to approximate the probability distribution, which is chosen as

$$g(\tau)=2500\tau e^{-50\tau}, \quad \tau\in[0, \ h].$$

Then, we define $g_0(s)=g(s)$ and construct a new vector $\boldsymbol{g}(s)=[g_0(s), g_1(s), \ldots, g_i(s), \ldots, g_\varrho(s)]^T$ with $\varrho\in\mathbb{N}$, where all the elements $g_i(s)$ are independent. According to [33], the basic principle of choosing $g_i(s)$ is that the chosen $g_i(s)$ should make the vector $\boldsymbol{g}(s)$ satisfy the property:

$$d\boldsymbol{g}(s)/ds=\mathcal{G}\boldsymbol{g}(s), \tag{7}$$

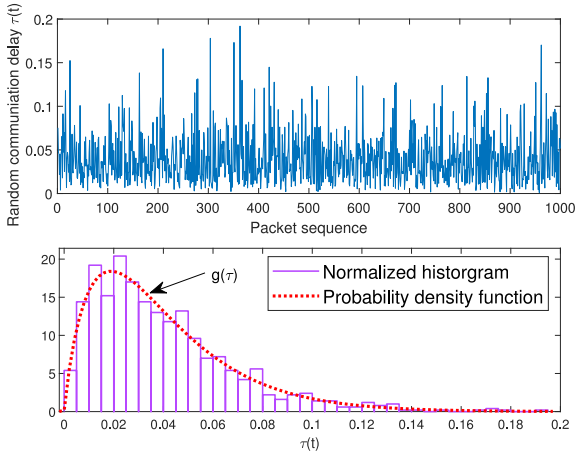

Fig. 2. Random delay $\tau(t)$ and its normalized histogram.

which means the elements $g_i(s)$ are the solutions of linear homogeneous differential equations with constant coefficients in the matrix $\mathcal{G} \in \mathbb{R}^{\varrho\times\varrho}$.

By utilizing the delay distribution information, the stochastic delayed signal $x_i(t-\tau)$ is modeled by a deterministic, distributed delay model $\int_{-h}^{0} g(s)x_i(t+s)ds$, which can be viewed as the mathematical expectation of $x_i(t-\tau)$. Then, $u_i^a(t)$ with the probability density of stochastic delays is expressed as:

$$u_i^a(t) = \mathcal{K}_i\mathcal{C}_i\int_{-h}^{0} g(s)x_i(t+s)ds + \lambda(t)\mathcal{K}_i\int_{-h}^{0} g(s)\varphi_i(t+s)ds. \tag{8}$$

Based on (8), the ith closed-loop LFC cyber-physical power system becomes

$$\begin{cases} \dot{x}_i(t) = \mathcal{A}_i x_i(t) + \mathcal{B}_i\mathcal{K}_i\mathcal{C}_i\int_{-h}^{0} g(s)x_i(t+s)ds \\ +\lambda(t)\mathcal{B}_i\mathcal{K}_i\int_{-h}^{0} g(s)\varphi_i(t+s)ds + \mathcal{F}_i\omega_i(t) \\ z_i(t) = \mathcal{C}_i x_i(t). \end{cases} \tag{9}$$

Remark 1: In this work, a new model of LFC system with random communication delays is established as a distributed delay system with kernel. In contrast to the conventional model based on an interval time-varying delay system only using the upper and lower bounds of delay, the delay probability density is taken into consideration in system modeling. Then, the presented distributed delay modeling approach has the potential to obtain less conservative results.

Remark 2: To describe the feature induced by random behaviors of adversaries, a Bernoulli variable $\lambda(t)$ is adopted to represent the control signal is attacked or not. Besides, the random feature caused by the delayed deceptive signal is also utilized in (8), which is not considered in [25], [26]. Thus, the presented model of deception attacks is more general than these existing results.

This article aims to design the controller (8) such that
1) The system (9) is mean-square asymptotically stable for $\omega_i(t) = 0$;
2) $\mathbb{E}\{\int_0^\infty z_i^{\mathsf{T}}(t)z_i(t)dt\} < \gamma_i^2\mathbb{E}\{\int_0^\infty \omega_i^{\mathsf{T}}(t)\omega_i(t)dt\}$ holds for $\omega_i(t) \neq 0$ and zero initial condition with a given $\gamma_i > 0$.

Before further proceeding, a useful lemma is given as below.

Lemma 1 [33]: For a symmetric matrix $\mathcal{Y} > 0 \in \mathbb{R}^{n\times n}$ and the vector $\boldsymbol{g}(s)$ given in (7), it gives

$$\int_{a_1}^{a_2} \mathbf{Sy}(\mathcal{Y}, x(s))ds \geq \mathbf{Sy}\left(\Omega\otimes\mathcal{Y}, \int_{a_1}^{a_2} G(s)x(s)ds\right) \tag{10}$$

with $\Omega^{-1} = \int_{a_1}^{a_2} \boldsymbol{g}(s)\boldsymbol{g}^{\mathsf{T}}(s)ds > 0$, $G(s) = \boldsymbol{g}(s)\otimes I_n$.

Remark 3: The Bessel-Legendre inequality in [29] uses Legendre polynomials to approximate the probability density, which leads to approximation error and further yields more conservative results. Different from this method, our method based on (10) can handle the probability density directly without any approximation error. Thus, less conservative results are obtained by the integral inequality (10) in Lemma 1 than the Bessel-Legendre inequality in [29].

III. Main Results

To derive the controller design conditions, the Lyapunov method is employed and the following Lyapunov-Krasovskii functional (LKF) is constructed as

$$\mathcal{V}(t) = \sum_{k=1}^{3}\mathcal{V}_k(t) \tag{11}$$

where

$$\mathcal{V}_1(t) = \xi_i^{\mathsf{T}}(t)P_i\xi_i(t), \quad \xi_i(t) = \left[x_i^{\mathsf{T}}(t) \quad \mathbb{G}_{xi}^{\mathsf{T}}(t) \quad \mathbb{G}_{\varphi i}^{\mathsf{T}}(t)\right]^{\mathsf{T}},$$

$$\mathcal{V}_2(t) = \int_{t-h}^{t} x_i^{\mathsf{T}}(s)[S_{1i} + (s-t+h)Y_{1i}]x_i(s)ds,$$

$$\mathcal{V}_3(t) = \int_{t-h}^{t} d_i^{\mathsf{T}}(s)[S_{2i} + (s-t+h)Y_{2i}]\varphi_i(s)ds,$$

$$\mathbb{G}_{xi}(t) \triangleq \int_{-h}^{0} G(s)x_i(t+s)ds, \quad \mathbb{G}_{\varphi i}(t) \triangleq \int_{-h}^{0} G(s)\varphi_i(t+s)ds,$$

$$G(s) \triangleq \boldsymbol{g}(s)\otimes I_n, g_0(s) = g(s), \boldsymbol{g}(s) = [g_0(s), \ldots, g_\varrho(s)]^{\mathsf{T}}.$$

Based on $G(s)$, $\mathbb{G}_{xi}(t)$ and $\mathbb{G}_{\varphi i}(t)$ defined in (11), one has

$$\int_{-h}^{0} g(s)x_i(t+s)ds = \mathcal{I}_1\mathbb{G}_{xi}(t), \tag{12}$$

$$\int_{-h}^{0} g(s)\varphi_i(t+s)ds = \mathcal{I}_2\mathbb{G}_{\varphi i}(t), \tag{13}$$

with $\mathcal{I}_1 = [I_5 \quad 0_{5,5\varrho}]$ and $\mathcal{I}_2 = [I_2 \quad 0_{2,2\varrho}]$.

By substituting (12) and (13) into (9), the ith closed-loop power system is further expressed as

$$\begin{cases} \dot{x}_i(t) = \mathcal{A}_i x_i(t) + \mathcal{B}_i\mathcal{K}_i\mathcal{C}_i\mathcal{I}_1\mathbb{G}_{xi}(t) \\ +\lambda(t)\mathcal{B}_i\mathcal{K}_i\mathcal{I}_2\mathbb{G}_{\varphi i}(t) + \mathcal{F}_i\omega_i(t) \\ z_i(t) = \mathcal{C}_i x_i(t) \end{cases} \tag{14}$$

To simplify the derivation, $\zeta_i(t)$ and $\mathbb{I}_a$ are defined as

$$\zeta_i(t) = [\zeta_{1i}(t)\zeta_{2i}(t)]^{\mathsf{T}}, \tag{15}$$

where

$$\zeta_{1i}(t) = \left[\dot{x}_i^{\mathsf{T}}(t)x_i^{\mathsf{T}}(t)x_i^{\mathsf{T}}(t-h)\varphi_i^{\mathsf{T}}(t)\varphi_i^{\mathsf{T}}(t-h)\right],$$

$$\zeta_{2i}(t) = \left[\mathbb{G}_{xi}^{\mathsf{T}}(t)\mathbb{G}_{\varphi i}^{\mathsf{T}}(t)\omega_i^{\mathsf{T}}(t)z_i^{\mathsf{T}}(t)\right].$$

Then, some sufficient H_∞ stability analysis criterions for the system (14) are provided in the following theorem.

Theorem 1: For given parameters h, ρ and controller gain $\mathcal{K}_i$, the system (14) is mean-square asymptotically stable with required H_∞ index γ_i, if there exist symmetric matrices P_i, $S_{1i} > 0$, $Y_{1i} > 0$, $S_{2i} > 0$, $Y_{2i} > 0$, $(i = 1, 2, \ldots, n)$, $0 < Z_i < \nu I$ and matrix X_i such that

$$\mathcal{P}_i > 0, \tag{17}$$

$$\Pi_i + \Lambda_i < 0, \tag{18}$$

for $i = 1, 2, \ldots, n$, where $\Omega = (\int_{-h}^{0} \boldsymbol{g}(s)\boldsymbol{g}^{\mathsf{T}}(s)ds)^{-1}$,

$$\mathcal{P}_i = P_i + diag\{0,\ \Omega \otimes S_{1i},\ \Omega \otimes S_{2i})\},$$

$$\Pi_i = \Gamma_i + \mathbf{He}(\mathscr{X}_i\mathscr{G}_i),\quad \Lambda_i = \mathbf{Sy}\Big(\nu(\mathcal{H}_i\mathcal{C}_i)^{\mathsf{T}}\mathcal{H}_i\mathcal{C}_i,\ \mathbb{I}_2\Big),$$

$$\begin{aligned}\Gamma_i = {} & \mathbf{He}\Big(\mathbb{J}^{\mathsf{T}}P_i\mathbb{Q}\Big) + \mathbf{Sy}(S_{1i} + hY_{1i},\ \mathbb{I}_2) - \mathbf{Sy}(S_{1i},\ \mathbb{I}_3)\\ & - \mathbf{Sy}(\Omega \otimes Y_{1i},\ \mathbb{I}_x) + \mathbf{Sy}(S_{2i} + hY_{2i} - Z_i,\ \mathbb{I}_4)\\ & - \mathbf{Sy}(S_{2i},\ \mathbb{I}_5) - \mathbf{Sy}\big(\Omega \otimes Y_{2i},\ \mathbb{I}_\varphi\big) - \gamma_i^2\mathbf{Sy}\big(I,\ \mathbb{I}_{8+2\varrho}\big)\\ & - \mathbf{Sy}\big(I,\ \mathbb{I}_{9+2\varrho}\big) + \mathbf{He}\Big(\mathbb{I}_{9+2\varrho}^{\mathsf{T}}\mathcal{C}_i\mathbb{I}_2\Big),\end{aligned}$$

$$\mathscr{G}_i = -\mathbb{I}_1 + \mathcal{A}_i\mathbb{I}_2 + \mathcal{B}_i\mathcal{K}_i\mathcal{C}_i\mathcal{I}_1\mathbb{I}_x + \bar{\lambda}\mathcal{B}_i\mathcal{K}_i\mathcal{I}_2\mathbb{I}_\varphi + \mathcal{F}_i\mathbb{I}_{8+2\varrho},$$

$$\mathscr{X}_i = (\mu_1 X_i\mathbb{I}_1 + \mu_2 X_i\mathbb{I}_2)^{\mathsf{T}},\ \widehat{\mathcal{G}}_1 = \mathcal{G} \otimes I_{(\varrho+1)4},\ \widehat{\mathcal{G}}_2 = \mathcal{G} \otimes I_{(\varrho+1)2},$$

$$\mathbb{J} = \begin{bmatrix}\mathbb{I}_2\\ \mathbb{I}_x\\ \mathbb{I}_\varphi\end{bmatrix},\ \mathbb{Q} = \begin{bmatrix}\mathbb{I}_1\\ G(0)\mathbb{I}_2 - G(-h)\mathbb{I}_3 - \widehat{\mathcal{G}}_1\mathbb{I}_x\\ G(0)\mathbb{I}_4 - G(-h)\mathbb{I}_5 - \widehat{\mathcal{G}}_2\mathbb{I}_\varphi\end{bmatrix},$$

$$\mathbb{I}_x = \begin{bmatrix}\mathbb{I}_6^{\mathsf{T}} & \cdots & \mathbb{I}_{6+\varrho}^{\mathsf{T}}\end{bmatrix}^{\mathsf{T}},\ \mathbb{I}_\varphi = \begin{bmatrix}\mathbb{I}_{7+\varrho}^{\mathsf{T}} & \cdots & \mathbb{I}_{7+2\varrho}^{\mathsf{T}}\end{bmatrix}^{\mathsf{T}}.$$

Proof: With the chosen LKF (11) for ith power system, by adopting Lemma 1, it leads to

$$\int_{-h}^{0} \mathbf{Sy}(Y_{1i}, x_i(t+s))ds \geq \mathbf{Sy}(\Omega \otimes Y_{1i}, \mathbb{G}_{xi}(t)), \tag{19}$$

$$\int_{-h}^{0} \mathbf{Sy}(Y_{2i}, \varphi_i(t+s))ds \geq \mathbf{Sy}\big(\Omega \otimes Y_{2i}, \mathbb{G}_{\varphi i}(t)\big). \tag{20}$$

In terms of (11), (19) and (20), one has

$$\begin{aligned}\mathcal{V}(t) \geq {} & \mathbf{Sy}(\mathcal{P}_i, \xi_i(t)) + \int_{-h}^{0} \mathbf{Sy}(Y_{1i}, x_i(t+s))ds\\ & + \int_{-h}^{0} \mathbf{Sy}(Y_{2i}, \varphi_i(t+s))ds.\end{aligned} \tag{21}$$

From $Y_{1i} > 0$, $Y_{2i} > 0$ and $\mathcal{P}_i > 0$, $\mathcal{V}(t) > 0$ is ensured. According to (7), it gives

$$\dot{\mathbb{G}}_{xi}(t) = G(0)x_i(t) - G(-h)x_i(t-h) - \widehat{\mathcal{G}}\mathbb{G}_{xi}(t), \tag{22}$$

$$\dot{\mathbb{G}}_{\varphi i}(t) = G(0)\varphi_i(t) - G(-h)\varphi_i(t-h) - \widehat{\mathcal{G}}\mathbb{G}_{\varphi i}(t). \tag{23}$$

Calculating the time derivative of $\mathcal{V}(t)$ and then subtracting $\gamma_i^2\omega_i^{\mathsf{T}}(t)\omega_i(t) - z_i^{\mathsf{T}}(t)z_i(t)$ yield

$$\begin{aligned}& \dot{\mathcal{V}}(t) - \gamma_i^2\omega_i^{\mathsf{T}}(t)\omega_i(t) + z_i^{\mathsf{T}}(t)z_i(t)\\ & = 2\xi_i^{\mathsf{T}}(t)P_i\dot{\xi}_i(t) - \gamma_i^2\omega_i^{\mathsf{T}}(t)\omega_i(t) + z_i^{\mathsf{T}}(t)z_i(t)\\ & \quad + \mathbf{Sy}(S_{1i} + hY_{1i}, x_i(t)) - \mathbf{Sy}(S_{1i}, x_i(t-h))\\ & \quad + \mathbf{Sy}(S_{2i} + hY_{2i}, \varphi_i(t)) - \mathbf{Sy}(S_{2i}, \varphi_i(t-h))\\ & \quad - \int_{-h}^{0} \mathbf{Sy}(Y_{1i}, x_i(t+s))ds - \int_{-h}^{0} \mathbf{Sy}(Y_{2i}, \varphi_i(t+s))ds.\end{aligned} \tag{24}$$

Using Lemma 1 to handle the integral terms in (24) gives

$$-\int_{-h}^{0} \mathbf{Sy}(Y_{1i}, x_i(t+s))ds \leq -\mathbf{Sy}(\Omega \otimes Y_{1i}, \mathbb{G}_{xi}(t)), \tag{25}$$

$$-\int_{-h}^{0} \mathbf{Sy}(Y_{2i}, \varphi_i(t+s))ds \leq -\mathbf{Sy}\big(\Omega \otimes Y_{2i}, \mathbb{G}_{\varphi i}(t)\big). \tag{26}$$

Based on Assumption (6) and $0 < Z_i < \nu I$, one gets

$$\nu x_i^{\mathsf{T}}(t)(\mathcal{H}_i\mathcal{C}_i)^{\mathsf{T}}\mathcal{H}_i\mathcal{C}_i x_i(t) - \varphi_i^{\mathsf{T}}(t)Z_i\varphi_i(t) \geq 0. \tag{27}$$

According to (15), (22) and (23), it results in

$$\xi_i(t) = \mathbb{J}\zeta_i(t),\quad \dot{\xi}_i(t) = \mathbb{Q}\zeta_i(t). \tag{28}$$

Combining (24), (25), (26) and (27), we obtain

$$\dot{\mathcal{V}}(t) - \gamma_i^2\omega_i^{\mathsf{T}}(t)\omega_i(t) + z_i^{\mathsf{T}}(t)z_i(t) \leq \mathbf{Sy}(\Gamma_i + \Lambda_i, \zeta_i(t)). \tag{29}$$

From the definition of $\zeta_i(t)$ in (15), the system (14) can be expressed as

$$\big(-\mathbb{I}_1 + \mathcal{A}_i\mathbb{I}_2 + \mathcal{B}_i\mathcal{K}_i\mathcal{C}_i\mathbb{I}_x + \lambda(t)\mathcal{B}_i\mathcal{K}_i\mathbb{I}_\varphi + \mathcal{F}_i\mathbb{I}_{8+2\varrho}\big)\zeta_i(t) = 0. \tag{30}$$

Taking the mathematical expectation of (30) yields

$$\begin{aligned}& \mathbb{E}\big\{\big(-\mathbb{I}_1 + \mathcal{A}_i\mathbb{I}_2 + \mathcal{B}_i\mathcal{K}_i\mathcal{C}_i\mathbb{I}_x + \bar{\lambda}\mathcal{B}_i\mathcal{K}_i\mathbb{I}_\varphi + \mathcal{F}_i\mathbb{I}_{8+2\varrho}\big)\zeta_i(t)\big\}\\ & = \mathbb{E}\{\mathscr{G}_i\zeta_i(t)\} = 0.\end{aligned} \tag{31}$$

Based on $\mathscr{X}_i = (\mu_1 X_i\mathbb{I}_1 + \mu_2 X_i\mathbb{I}_2)^{\mathsf{T}}$ and (31), it leads to

$$\mathbb{E}\Big\{\zeta_i^{\mathsf{T}}(t)\mathscr{X}_i\mathscr{G}_i\zeta_i(t)\Big\} = 0. \tag{32}$$

According to (29), (32) and $\Pi_i + \Lambda_i < 0$ from (18), it gives

$$\begin{aligned}& \mathbb{E}\Big\{\dot{\mathcal{V}}(t) - \gamma_i^2\omega_i^{\mathsf{T}}(t)\omega_i(t) + z_i^{\mathsf{T}}(t)z_i(t)\Big\}\\ & \leq \mathbb{E}\Big\{\zeta_i^{\mathsf{T}}(t)(\Pi_i + \Lambda_i)\zeta_i(t)\Big\} < 0.\end{aligned} \tag{33}$$

By integrating (33) over $[0, \infty)$, one has

$$\mathbb{E}\{\mathcal{V}(\infty) - \mathcal{V}(0)\} < \mathbb{E}\left\{\int_0^\infty \Big(\gamma_i^2\omega_i^{\mathsf{T}}(t)\omega_i(t) - z_i^{\mathsf{T}}(t)z_i(t)\Big)dt\right\}. \tag{34}$$

If $\omega_i(t) = 0$, one has $\mathbb{E}\{\dot{\mathcal{V}}(t)\} < 0$ from (33). Hence the system (9) is mean-square asymptotically stable. Moreover, for $\omega_i(t) \neq 0$ and $x(0) = 0$, one gets $\mathbb{E}\{\int_0^\infty z_i^{\mathsf{T}}(t)z_i(t))dt\} \leq \mathbb{E}\{\gamma_i^2\int_0^\infty \omega_i^{\mathsf{T}}(t)\omega_i(t)dt\}$ from (34). ■

$$\mathbb{I}_a = \begin{cases}\big[0_{5,5(a-1)} \quad I_5 \quad 0_{5,5(3-a)} \quad 0_{5,4} \quad 0_{5,5(1+\varrho)} \quad 0_{5,2(1+\varrho)} \quad 0_{5,4}\big], & a = 1, 2, 3\\ \big[0_{2,15} \quad 0_{2,5(a-4)} \quad I_2 \quad 0_{2,5(5-a)} \quad 0_{2,5(1+\varrho)} \quad 0_{2,2(1+\varrho)} \quad 0_{2,4}\big], & a = 4, 5\\ \big[0_{5,15} \quad 0_{5,4} \quad 0_{5,5(a-6)} \quad I_5 \quad 0_{5,5(6+\varrho-a)} \quad 0_{5,2(1+\varrho)} \quad 0_{5,4}\big], & a = 6, \ldots, 6+\varrho\\ \big[0_{2,15} \quad 0_{2,4} \quad 0_{2,5(1+\varrho)} \quad 0_{2,2(a-7-\varrho)} \quad I_2 \quad 0_{2,2(7+2\varrho-a)} \quad 0_{2,4}\big], & a = 7+\varrho, \cdots, 7+2\varrho\\ \big[0_{2,15} \quad 0_{2,4} \quad 0_{2,5(1+\varrho)} \quad 0_{2,2(1+\varrho)} \quad 0_{2,2(8+2\varrho-a)} \quad I_2 \quad 0_{2,2(9+2\varrho-a)}\big], & a = 8+2\varrho, \ldots, 9+2\varrho\end{cases} \tag{16}$$

Remark 4: In terms of the condition (17), $P_i > 0$ is not necessary to make the selected LKF (11) positive. Thus, this relaxation could lead to less conservative stability conditions than some existing conditions requiring $P_i > 0$.

According to the stability results in Theorem 1, the controller design conditions of system (14) are derived in Theorem 2.

Theorem 2: For given scalars μ_1, μ_2, h, ρ, the system (14) is asymptotically stable in mean-square with required H_∞ index γ_i, if there exist symmetric matrices $\tilde{P}_i$, $\tilde{S}_{1i} > 0$, $\tilde{Y}_{1i} > 0$, $\tilde{S}_{2i} > 0$, $\tilde{Y}_{2i} > 0$, $\mathcal{Z}_i > \nu^{-1} I$ and matrices N_i, M_i, $\mathcal{L}_i$ such that

$$\tilde{\mathcal{P}}_i > 0, \tag{35}$$

$$\begin{bmatrix} \tilde{\Pi}_i & \nu \mathbb{I}_2^{\mathsf{T}} M_i (\mathcal{H}_i \mathcal{C}_i)^{\mathsf{T}} \\ * & -\nu I \end{bmatrix} < 0, \tag{36}$$

$$\begin{bmatrix} -\epsilon I & (N_i \mathcal{C}_i - \mathcal{C}_i M_i)^{\mathsf{T}} \\ * & -I \end{bmatrix} < 0, \tag{37}$$

for $i = 1, 2, \ldots, n$, where

$$\begin{aligned}
\tilde{\mathcal{P}}_i &= \tilde{P}_i + diag\Big\{0,\ \Omega \otimes \tilde{S}_{1i},\ \Omega \otimes \tilde{S}_{2i})\Big\}, \\
\tilde{\Gamma}_i &= \mathbf{He}\Big(\mathbb{J}^{\mathsf{T}} \tilde{P}_i \mathbb{Q}\Big) + \mathbf{Sy}\Big(\tilde{S}_{1i} + h\tilde{Y}_{1i}, \mathbb{I}_2\Big) - \mathbf{Sy}\Big(\tilde{S}_{1i}, \mathbb{I}_3\Big) \\
&\quad - \mathbf{Sy}\big(\Omega \otimes \tilde{Y}_{1i}, \mathbb{I}_x\big) + \mathbf{Sy}\Big(\tilde{S}_{2i} + h\tilde{Y}_{2i} + \rho^2 \mathcal{Z}_i - 2\rho N_i, \mathbb{I}_4\Big) \\
&\quad - \mathbf{Sy}\Big(\tilde{S}_{2i}, \mathbb{I}_5\Big) - \mathbf{Sy}\big(\Omega \otimes \tilde{Y}_{2i}, \mathbb{I}_\varphi\big) - \gamma_i^2 \mathbf{Sy}\big(I, \mathbb{I}_{8+2\varrho}\big) \\
&\quad - \mathbf{Sy}\big(I, \mathbb{I}_{9+2\varrho}\big) + \mathbf{He}(\mathbb{I}_{9+2\varrho}^{\mathsf{T}} \mathcal{C}_i M_i \mathbb{I}_2), \\
\tilde{\mathcal{G}}_i &= -M_i \mathbb{I}_1 + \mathcal{A}_i M_i \mathbb{I}_2 + \mathcal{B}_i \mathcal{L}_i \mathcal{C}_i \mathbb{I}_x + \bar{\lambda} \mathcal{B}_i \mathcal{L}_i \mathbb{I}_\varphi + \mathcal{F}_i \mathbb{I}_{8+2\varrho}, \\
\tilde{\mathcal{X}}_i &= (\mu_1 \mathbb{I}_1 + \mu_2 \mathbb{I}_2)^{\mathsf{T}}, \quad \tilde{\Pi}_i = \tilde{\Gamma}_i + \mathbf{He}\Big(\tilde{\mathcal{X}}_i \tilde{\mathcal{G}}_i\Big).
\end{aligned}$$

Moreover, the controller gains are computed by $\mathcal{K}_i = \mathcal{L}_i N_i^{-1}$.

Proof: Adopting Schur complement to (18) leads to

$$\begin{bmatrix} \Pi_i & \nu \mathbb{I}_2^{\mathsf{T}} (\mathcal{H}_i \mathcal{C}_i)^{\mathsf{T}} \\ * & -\nu I \end{bmatrix} < 0. \tag{38}$$

Define $M_i = X_i^{-1}$, $\tilde{P}_i = (I_{2(\varrho+1)+1} \otimes M_i) P_i (I_{2(\varrho+1)+1} \otimes M_i)$, $\tilde{S}_{1i} = M_i S_{1i} M_i$, $\tilde{Y}_{1i} = M_i Y_{1i} M_i$, $\tilde{S}_{2i} = N_i S_{2i} N_i$, $\tilde{Y}_{2i} = N_i Y_{2i} N_i$, $N_i \mathcal{C}_i = \mathcal{C}_i M_i$ and $\mathcal{L}_i \mathcal{C}_i = \mathcal{K}_i \mathcal{C}_i M_i$.

Left- and right-multiplying (38) with $\mathscr{M}_i = diag\{M_i, M_i, M_i, N_i, N_i, I_{\varrho+1} \otimes M_i, I_{\varrho+1} \otimes N_i, I, I\}$ and its transpose, one has

$$\begin{bmatrix} \hat{\Pi}_i & \nu \mathbb{I}_2^{\mathsf{T}} M_i (\mathcal{H}_i \mathcal{C}_i)^{\mathsf{T}} \\ * & -\nu I \end{bmatrix} < 0, \tag{39}$$

where $\hat{\Pi}_i = \hat{\Gamma}_i + \mathbf{He}(\tilde{\mathcal{X}}_i \tilde{\mathcal{G}}_i)$,

$$\begin{aligned}
\hat{\Gamma}_i &= \mathbf{He}\Big(\mathbb{J}^{\mathsf{T}} \tilde{P}_i \mathbb{Q}\Big) + \mathbf{Sy}\Big(\tilde{S}_{1i} + h\tilde{Y}_{1i}, \mathbb{I}_2\Big) - \mathbf{Sy}\Big(\tilde{S}_{1i}, \mathbb{I}_3\Big) \\
&\quad - \mathbf{Sy}\big(\Omega \otimes \tilde{Y}_{1i}, \mathbb{I}_x\big) + \mathbf{Sy}\Big(\tilde{S}_{2i} + h\tilde{Y}_{2i} - N_i^T Z_i N_i, \mathbb{I}_4\Big) \\
&\quad - \mathbf{Sy}\Big(\tilde{S}_{2i}, \mathbb{I}_5\Big) - \mathbf{Sy}\big(\Omega \otimes \tilde{Y}_{2i}, \mathbb{I}_\varphi\big) - \gamma_i^2 \mathbf{Sy}\big(I, \mathbb{I}_{8+2\varrho}\big) \\
&\quad - \mathbf{Sy}\big(I, \mathbb{I}_{9+2\varrho}\big) + \mathbf{He}\Big(\mathbb{I}_{9+2\varrho}^{\mathsf{T}} \mathcal{C}_i M_i \mathbb{I}_2\Big).
\end{aligned}$$

Utilizing the inequality $-N_i^{\mathsf{T}} Z_i N_i \le \rho^2 Z_i^{-1} - 2\rho N_i$ to (39) yields (36) by introducing a novel variable matrix $\mathcal{Z}_i = Z_i^{-1}$.

It is infeasible to solve the equation $N_i \mathcal{C}_i = \mathcal{C}_i M_i$ since it is not a strict inequality. Then the problem of tackling the nonlinear item $X_i^{\mathsf{T}} \mathcal{B}_i \mathcal{K}_i \mathcal{C}_i$ in Theorem 1 can be transformed as a *W-problem* [35].

In terms of $N_i \mathcal{C}_i = \mathcal{C}_i M_i$, it yields

$$(N_i \mathcal{C}_i - \mathcal{C}_i M_i)^{\mathsf{T}} (N_i \mathcal{C}_i - \mathcal{C}_i M_i) = 0. \tag{40}$$

By using Schur complement to (40), one can get

$$\begin{bmatrix} -\epsilon I & (N_i \mathcal{C}_i - \mathcal{C}_i M_i)^{\mathsf{T}} \\ * & -I \end{bmatrix} < 0, \tag{41}$$

which equals the condition (37) with a sufficient small constant $\epsilon > 0$. Then, the proof is fulfilled. ■

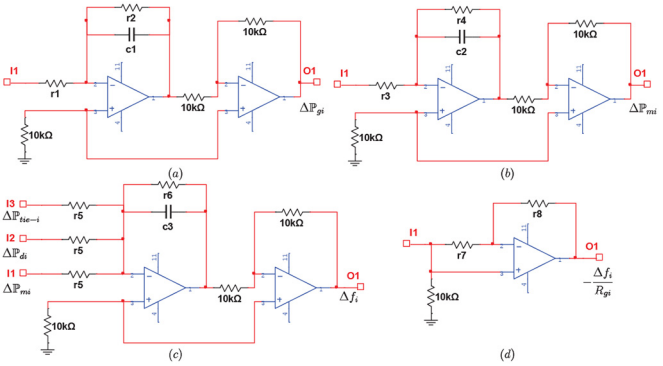

Fig. 3. Circuital implementation of (a) governor; (b) turbine; (c) power generator and (d) droop constant for Area 1.

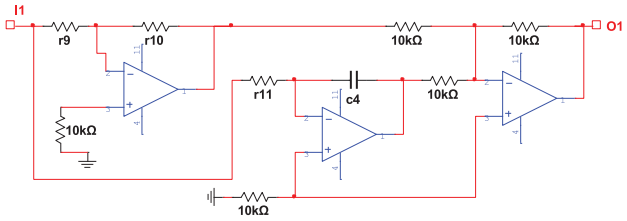

Fig. 4. Circuital implementation of the controller for Area 1.

IV. Circuital Implementation

In this section, a specific circuital execution method is used to imitate the considered LFC power system, where the system components and controller are realized by some equivalent analogy circuits based on resistors, capacitors and operational amplifiers. For simplification of presentation, the first control area ($i = 1$) of a multi-area NPS with three control areas is discussed below.

It is noted that the dynamics of system components are described via some first-order inertial elements in Fig. 1. By defining the parameters as: $r_1 = r_2$, $\mathbb{T}_{gi} = r_1 c_1$, $r_3 = r_4$, $\mathbb{T}_{ti} = r_3 c_2$, $\mathbb{D}_i = \frac{r_6}{r_5}$, $\mathbb{M}_i = r_5 c_3$, the equivalent analogy circuits of them are shown in Fig. 3 (a), (b) and (c), respectively. The droop constant can be viewed as a proportion element, and its equivalent analogy circuit is shown in Fig. 3 (d) by choosing $\frac{1}{\mathbb{R}_{gi}} = \frac{r_8}{r_7}$.

The circuital realization of the PI controller is drawn in Fig. 4, where a proportion circuit, an integration circuit and an adding circuit are used to represent $u_i(t) = \mathcal{K}_{Pi} ACE_i(t) + \mathcal{K}_{Ii} \int ACE_i(t) dt$ with $\mathcal{K}_{Pi} = \frac{r_{10}}{r_9}$ and $\mathcal{K}_{Ii} = \frac{1}{r_{11} c_4}$.

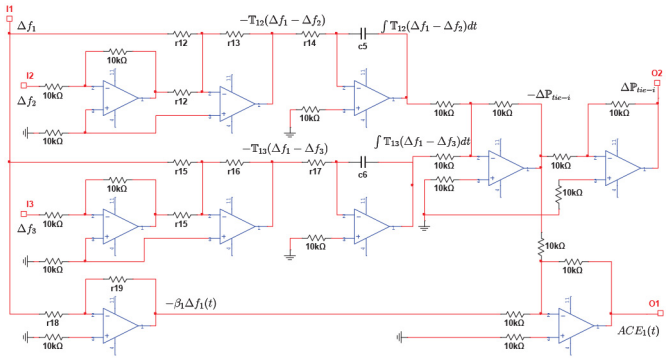

Fig. 5. Circuital implementation of $ACE_i(t)$ for Area 1.

TABLE I
THE VALUES OF PARAMETERS

Area	1	2	3
$\mathbb{D}$	0.015	0.014	0.015
$\mathbb{M}$	0.1667	0.12	0.2
$\mathbb{T}_g$	0.08	0.06	0.07
$\mathbb{T}_t$	0.4	0.36	0.42
$\mathbb{R}_g$	3	3	3.3
β	0.3483	0.3473	0.318
	$\mathbb{T}_{12}=0.2$	$\mathbb{T}_{13}=0.25$	$\mathbb{T}_{23}=0.12$

The signal $ACE_i(t)$ of (2) shown in Fig. 5 is the sum of the signal $\beta_i\Delta f_i(t)$ and the signal $\Delta\mathbb{P}_{tie-i}(t)$, which can be realized by adding circuit with OA and some resistors with the same resistance values. The signal $\beta_i\Delta f_i(t)$, the product of the bias β_i and $\Delta f_i(t)$, can be achieved by proportion circuit with $\beta_i=\frac{r_{19}}{r_{18}}$. The signal $\Delta\mathbb{P}_{tie-i}(t)$ equals to the sum of $\int \mathbb{T}_{12}(\Delta f_1(t)-\Delta f_2(t))$ and $\int \mathbb{T}_{13}(\Delta f_1(t)-\Delta f_3(t))$, which can be derived by integration circuits with $r_{14}c_5=1$ and $r_{17}c_6=1$. Moreover, the signal $\mathbb{T}_{12}(\Delta f_1(t)-\Delta f_2(t))$ is obtained by subtraction circuit and proportion circuit with $\mathbb{T}_{12}=\frac{r_{13}}{r_{12}}$. The same process of deriving the signal $\mathbb{T}_{13}(\Delta f_1(t)-\Delta f_3(t))$ is executed with $\mathbb{T}_{13}=\frac{r_{16}}{r_{15}}$.

Remark 5: The equivalent analogy circuits for power systems can be viewed as low-cost simulators, which are used to test the effectiveness of the proposed control method. This is helpful for avoiding the serious hazard induced by potential drawbacks of designed controller to expensive devices of practical systems. Meanwhile, the cost of testing can be saved dramatically.

V. EXAMPLE

The parameters of the considered NPS are borrowed from [34], which are presented in Table I.

In this example, the random transmission delays shown in Fig. 2 are considered. In order to correspond to the form of $\int_{-h}^{0} g(s)x(t+s)ds$ in the derivations, $g(\tau)$ is written as $g(s)=g_0(s)=-2500se^{50s}$, $s\in[-h,\ 0]$. For $\varrho=1$, to construct the vector $\boldsymbol{g}(s)$ satisfying (7), another term $g_1(s)=-50e^{50s}$ is chosen. Then, the vector $\boldsymbol{g}(s)$ and corresponding parameters are given as

$$\boldsymbol{g}(s)=\begin{bmatrix}-2500se^{50s}\\ -50e^{50s}\end{bmatrix},\ \mathcal{G}=\begin{bmatrix}50 & 50\\ 0 & 50\end{bmatrix},\ \Omega=\begin{bmatrix}0.16 & 0.08\\ 0.08 & 0.08\end{bmatrix}.$$

TABLE II
THE VALUES OF CIRCUIT ELEMENTS

Parameters	Values	Parameters	Values	Parameters	Values
$r_1=r_2$	$10K\Omega$	r_8	$10K\Omega$	c_5	$100\mu F$
c_1	$8\mu F$	r_9	$10K\Omega$	r_{15}	$10K\Omega$
$r_3=r_4$	$10K\Omega$	r_{10}	$6.718K\Omega$	r_{16}	$2.5K\Omega$
c_2	$40\mu F$	r_{11}	$10K\Omega$	r_{17}	$30K\Omega$
r_5	$10K\Omega$	c_4	$0.338mF$	c_6	$100\mu F$
r_6	$0.15K\Omega$	r_{12}	$10K\Omega$	r_{18}	$10K\Omega$
c_3	$16.67\mu F$	r_{13}	$2K\Omega$	r_{19}	$3.483K\Omega$
r_7	$30K\Omega$	r_{14}	$10K\Omega$		

For the given matrix $\mathcal{H}_i=I_2$, and considering the deception attack signal $\varphi_i(t)=\begin{bmatrix}tanh(y_{i1}(t))\\ tanh(y_{i2}(t))\end{bmatrix}$, we have $\|\varphi_i(t)\|_2\le\|\mathcal{H}_i\mathcal{C}_ix_i(t)\|_2$ based on $|tanh(y_{i1}(t))|\le 1$ and $|tanh(y_{i2}(t))|\le 1$. Under the given H_∞ index $\gamma_i=20$, by choosing $\epsilon=0.01$, $\mu_1=0.1$, $\mu_2=0.5$, $\rho=0.3$ and $\nu=10$, the controller gains of three power systems solved by Theorem 2 for different probabilities of the attack occurrence $\bar{\lambda}=0.5$ are derived as:

$$\mathcal{K}_1=\begin{bmatrix}0.6718, -0.2956\end{bmatrix},$$
$$\mathcal{K}_2=\begin{bmatrix}0.7781, -0.3324\end{bmatrix},$$
$$\mathcal{K}_3=\begin{bmatrix}0.8797, -0.5440\end{bmatrix}.$$

The control system is simulated via circuital realization method in Simulink/MATLAB. The system components and the PI controller can be realized by equivalent electrical circuits. The professional **Simcape** toolbox of Simulink is used to realize the governor, turbine and power generator of Area 1, which is given in Fig. 6. Due to page limitation, the other simulation diagrams are omitted here. The communication network is executed by a variable delay module and a random number module generating the random delay given by Simulink. According to Section IV, the values of resistors and capacitors of analogy circuits for the Area 1 are given in Table II. Due to page limitation, the other two areas are omitted here.

In the simulation, the sampling period is $0.01s$ and the initial condition is zero. The following two different cases of load variations are considered.

Case 1: The load variations for three control areas are $\Delta\mathbb{P}_{d1}(t)=0.1sin(0.5t)$, $\Delta\mathbb{P}_{d2}(t)=0.1sin(\pi t)$ and $\Delta\mathbb{P}_{d3}(t)=0.1sin(1.5t)$ for $0<t<5s$; otherwise, $\Delta\mathbb{P}_{di}(t)=0$ for $t\ge 5s$ and $i=1,2,3$.

Case 2: The load variations for three control areas are $\Delta\mathbb{P}_{di}(t)=0.1$ for $0<t<2s$; $\Delta\mathbb{P}_{di}(t)=-0.1$ for $2\le t<4s$; otherwise, $\Delta\mathbb{P}_{di}(t)=0$ for $t\ge 4s$ and $i=1,2,3$.

For the considered deception attacks and the load variations in **Case 1**, the frequency trajectories by using the designed controller gains are drawn in Fig. 7. Meanwhile, the corresponding curves for **Case 2** are drawn in Fig. 8. These figures denote that for the above two different situations of load variations, the designed controllers are effective for maintaining the system frequencies to be stable even when control signals are attacked by deceptive data.

To show the advantages of the proposed method over some existing ones, three groups of comparison results are provided as below.

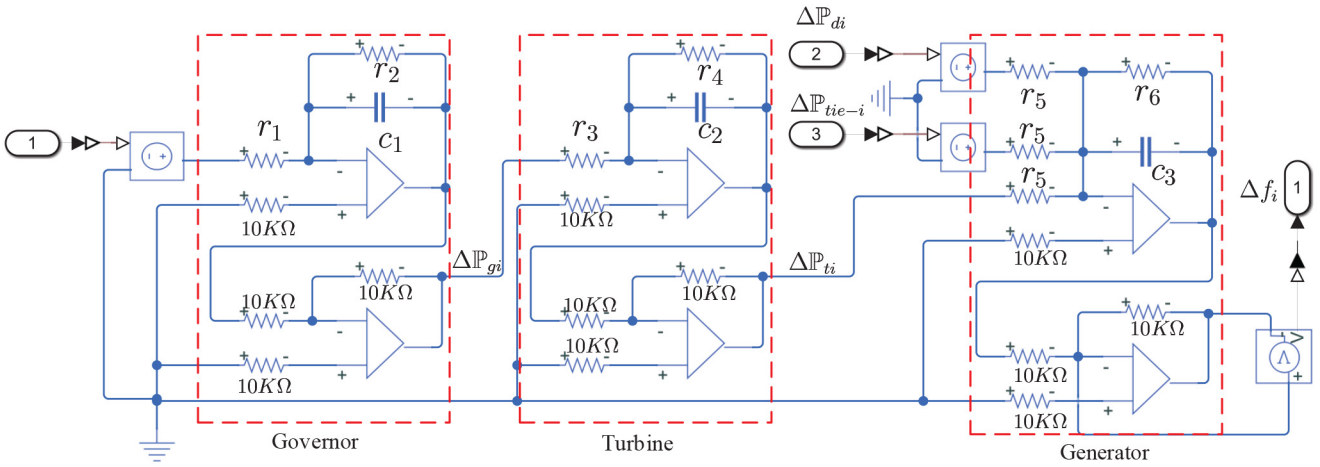

Fig. 6. The diagram for governor, turbine and power generator of Area 1 via circuital realization in Simulink/MATLAB.

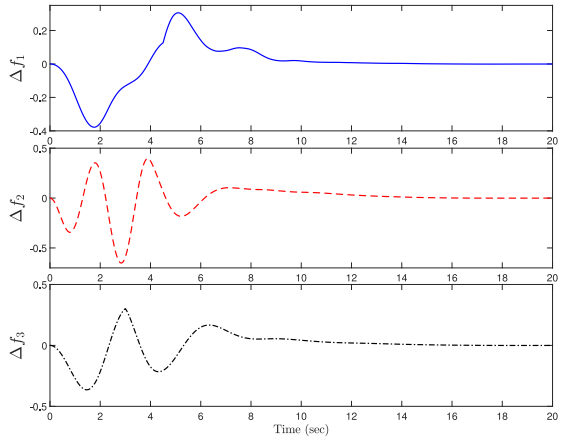

Fig. 7. Responses of the frequency for three areas under $\bar{\lambda} = 0.5$ and load variations in **Case 1**.

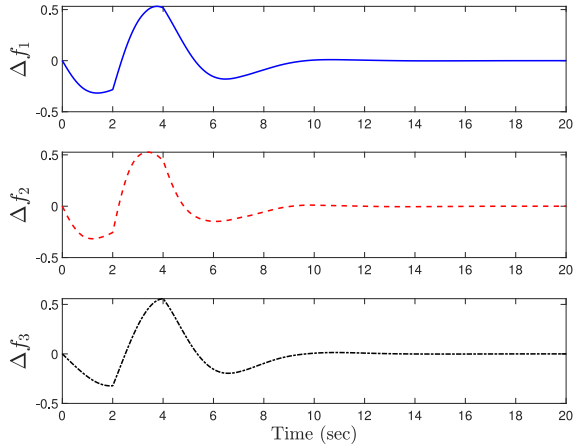

Fig. 8. Responses of the frequency for three areas under $\bar{\lambda} = 0.5$ and load variations in **Case 2**.

A. The First Comparison Group

The following comparison further shows the better control performance of our designed controller against deception attacks than the existing controller. Two cases are considered:

Case 3: The controller is designed without taking into account the deception attacks, which is called a '**standard**' controller. In this case, the controller design conditions can be obtained by removing the terms related to $\varphi_i(t)$. With the above parameters and $\bar{\lambda} = 0.3$, the controller gains are derived as:

$$\mathcal{K}_1 = [1.7601, -0.5126],$$
$$\mathcal{K}_2 = [2.1556, -0.3525],$$
$$\mathcal{K}_3 = [2.5467, -1.2538];$$

Case 4: The controller is designed by our method considering the deception attacks, which is called a '**resilient**' controller. Namely, the designed resilient controller is able to ensure the system stability even if the system is attacked. In this case, with $\bar{\lambda} = 0.3$ and the same parameters used in **Case 3**, the controller gains solved by Theorem 2 are:

$$\mathcal{K}_1 = [0.8119, -0.3225],$$
$$\mathcal{K}_2 = [0.9781, -0.3599],$$
$$\mathcal{K}_3 = [1.0859, -0.5885].$$

In this simulation, the load disturbances are taken as $\Delta\mathbb{P}_{d1}(t) = 0.1cos(\pi t)e^{-0.5t}$, $\Delta\mathbb{P}_{d2}(t) = 0.1sin(\pi t)e^{-0.5t}$ and $\Delta\mathbb{P}_{d3}(t) = 0.1e^{-0.5t}$ for $0 < t < 8s$ ($\omega(t) = 0$ for $t \geq 8s$) for three areas. The responses of system frequencies in **Case 3** and **Case 4** are drawn in Fig. 9 and Fig. 10, respectively. By comparing the curves in Fig. 9 and Fig. 10, it is observed that our proposed controller considering the deception attacks (**Case 4**) can produce better control performance than the controller designed without considering the deception attacks (**Case 4**). From Fig. 9, it is seen that the standard controller is not able to stabilize the system frequencies when the transmitted signals are attacked by injecting some deceptive data. However, Fig. 10 shows our designed resilient controller can still guarantee the stability of system frequencies even deception attacks happen. This means that our proposed control strategy is resilient to the deception attacks and can outperform the standard control method.

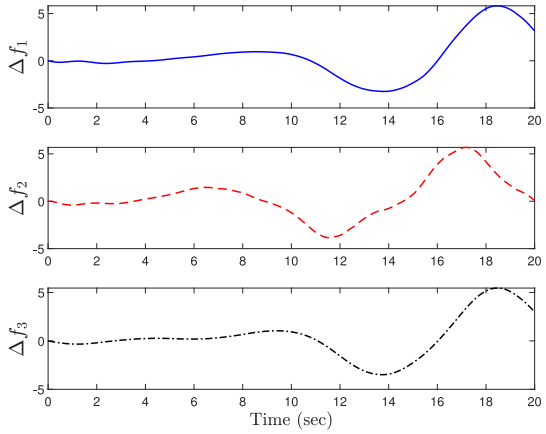

Fig. 9. **Case 3**: Responses of the frequency for three areas with 'standard controller.'

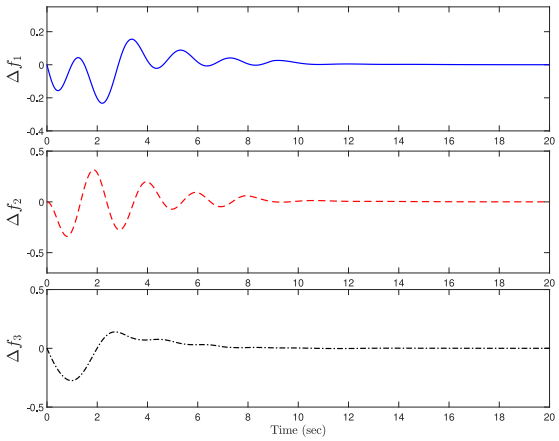

Fig. 10. **Case 4**: Responses of the frequency for three areas with our 'resilient controller.'

TABLE III
COMPARISON OF THE MINIMUM H_∞ INDEX γ USING DIFFERENT DELAY HANDLING METHODS

Random delay	γ	Area 1	Area 2	Area 3
$h = 0.1$	Method in [15]	8.3924	7.8852	8.5073
	Our method	7.9225	7.3720	8.0383
$h = 0.2$	Method in [15]	10.5156	9.6582	10.5434
	Our method	8.1678	7.7804	8.2373
$h = 0.3$	Method in [15]	12.6137	11.2883	11.6981
	Our method	8.5040	8.1621	8.4756

B. The Second Comparison Group

To illustrate the advantage of the delay modeling approach based on probability density, the comparison results of the H_∞ index for three power systems obtained by our approach and the conventional interval time-varying delay approach in [15] are given in Table III, where three different random delay cases are considered.

To be specific, the first case is $g(s) = -10000se^{100s}$, $s \in [-h,\ 0]$ and $h = 0.1$; the second case is $g(s) = -2500se^{50s}$, $s \in [-h,\ 0]$ and $h = 0.2$; the third case is $g(s) = -1110se^{33s}$, $s \in [-h,\ 0]$ and $h = 0.3$. And the second case is the same with the random delay given in Fig. 2.

TABLE IV
COMPARISON OF $\wp$ AND THE MINIMUM H_∞ INDEX γ UNDER DIFFERENT METHODS

γ	$\wp$	Area 1	Area 2	Area 3
Method in [29] with $\varrho = 1$	325	10.5990	10.1752	10.8573
Method in [29] with $\varrho = 3$	1035	9.6345	9.3506	9.7195
Method in [29] with $\varrho = 5$	2145	8.5621	8.1213	8.8802
Our method with $\varrho = 1$	325	8.1678	7.7804	8.2373

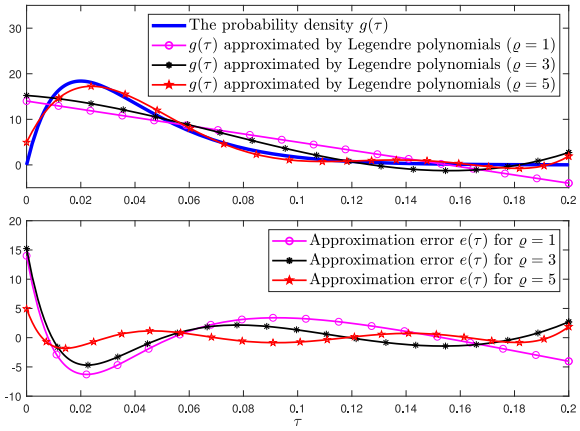

Fig. 11. $g(\tau)$, $\hat{g}(\tau)$ and $e(\tau) = \hat{g}(\tau) - g(\tau)$ with $\varrho = 1, 3, 5$.

According to this table, all the optimized γ_i of three control areas obtained by our method are smaller than the results derived by traditional interval time-varying delay approach, which indicates better stability performance will be achieved. Specifically, for $h = 0.1$ and $i = 1, 2, 3$, the values of γ_i are reduced by 5.6%, 6.5% and 5.5%; for $h = 0.2$ and $i = 1, 2, 3$, the reductions of the values of γ_i are 22.3%, 19.4% and 21.9%; for $h = 0.3$ and $i = 1, 2, 3$, the corresponding reductions are 32.6%, 27.7% and 27.5%. In addition, it is also seen that the corresponding values of γ_i increase as the growth of the values of delay bound h.

C. The Third Comparison Group

To show the merit of our approach based on Lemma 1 to handle the distributed delay with kernel, the comparison results of the H_∞ index derived by our method and the Bessel-Legendre inequality in [29] are obtained in Table IV.

The second case of random delay with $h = 0.2$ in the above second comparison group is considered here. Following the method in [29], we utilize Legendre polynomials to approximate the distributed kernel $g(\tau)$. For given ϱ, $g(\tau)$ can be approximated by $\hat{g}(\tau)$:

$$\hat{g}(\tau) = \sum_{i=0}^{\varrho} \frac{2i+1}{h} \int_0^h g(\tau)\mathbb{L}_i\Big(\frac{\tau}{h}\Big)d\tau,$$

where $\mathbb{L}_i(\frac{\tau}{h}) = (-1)^i \sum_{j=0}^{i}(-1)^j\binom{i}{j}\binom{i+j}{j}(\frac{\tau}{h})^j$. The figures of the distributed kernel $g(\tau)$ and its approximation $\hat{g}(\tau)$ with different ϱ are shown in Fig. 11. Furthermore, the optimized H_∞ index γ and the number of decision variables ($\wp = \frac{5}{2}(2\varrho + 3)(1 + 5(2\varrho + 3))$) in P_i with our method and the method in [29] are shown in Table IV. In terms of

this figure and Table IV, it is indicated that $\wp$ increases and the approximation error $e(\tau)$ decreases as the growth of ϱ. Meanwhile, one can also observe that our approach needs fewer decision variables to deal with the random delay and deception attack without any approximation error and leads to better H_∞ performance than the existing approach in [29].

Based on these comparison results, it is shown that the proposed LFC method for NPSs subject to random delay and deception attacks in this manuscript is more effective than some existing methods.

VI. Conclusion

This work studied the decentralized H_∞ secure LFC of NPSs with random communication delays and deception attacks. A novel model of random transmission delays has been presented by using the delay probability density. Based on this model, the normal control signals and deception attacks were represented as two distributed delay terms, in which the probability density is treated as the distributed delay kernel. Then, new sufficient probability-density-dependent conditions were proposed by Lyapunov method to design the decentralized H_∞ secure controller to maintain the system frequencies. The dynamics of power system were realized by electrical circuit systems, which were executed by the professional Simcape toolbox of Simulink/MATLAB. The simulation examples demonstrated the effectiveness of the developed approach. In addition, how to extend the developed approach to handle the LFC issue of NPSs with nonlinear dynamics or integrated with wind power and solar power deserves further investigations in the future.

References

[1] C. Zhao, W. Sun, J. Wang, Q. Li, D. Mu, and X. Xu, "Distributed cooperative secondary control for islanded microgrid with Markov time-varying delays," *IEEE Trans. Energy Convers.*, vol. 34, no. 4, pp. 2235–2247, Dec. 2019.

[2] K. Xiahou, Y. Liu, and Q. Wu, "Robust load frequency control of power systems against random time-delay attacks," *IEEE Trans. Smart Grid*, vol. 12, no. 1, pp. 909–911, Jan. 2021.

[3] Y. Wu, Z. Wei, J. Weng, X. Li, and R. H. Deng, "Resonance attacks on load frequency control of smart grids," *IEEE Trans. Smart Grid*, vol. 9, no. 5, pp. 4490–4502, Sep. 2018.

[4] F. Yang, J. He, and Q. Pan, "Further improvement on delay-dependent load frequency control of power systems via truncated B–L inequality," *IEEE Trans. Power Syst.*, vol. 33, no. 5, pp. 5062–5071, Sep. 2018.

[5] J. He, Y. Liang, X. Hao, F. Yang, and Q. Pan, "A quadratic convex framework with bigger freedom for the stability analysis of a cyber-physical microgrid system," *Sci. China Inf. Sci.*, 2022, doi: 10.1007/s11432-021-3433-8.

[6] C. Peng, J. Zhang, and H. Yan, "Adaptive event-triggering H_∞ load frequency control for network-based power systems," *IEEE Trans. Ind. Electron.*, vol. 65, no. 2, pp. 1685–1694, Feb. 2018.

[7] Y. Liu, Y. Chen, and M. Li, "Dynamic event-based model predictive load frequency control for power systems under cyber attacks," *IEEE Trans. Smart Grid*, vol. 12, no. 1, pp. 715–725, Jan. 2021.

[8] E. Tian and C. Peng, "Memory-based event-triggering H_∞ load frequency control for power systems under deception attacks," *IEEE Trans. Cybern.*, vol. 50, no. 11, pp. 4610–4618, Nov. 2020.

[9] T. Yang, Y. Zhang, W. Li, and A. Y. Zomaya, "Decentralized networked load frequency control in interconnected power systems based on stochastic jump system theory," *IEEE Trans. Smart Grid*, vol. 11, no. 5, pp. 4427–4439, Sep. 2020.

[10] Y. Mi, Y. Fu, C. Wang, and P. Wang, "Decentralized sliding mode load frequency control for multi-area power systems," *IEEE Trans. Power Syst.*, vol. 28, no. 4, pp. 4301–4309, Nov. 2013.

[11] S. Yan, S. K. Nguang, and Z. Gu, "H_∞ weighted integral event-triggered synchronization of neural networks with mixed delays," *IEEE Trans. Ind. Informat.*, vol. 17, no. 4, pp. 2365–2375, Apr. 2021.

[12] M. H. Khooban, T. Niknam, F. Blaabjerg, and T. Dragicevic, "A new load frequency control strategy for micro-grids with considering electrical vehicles," *Elect. Power Syst. Res.*, vol. 143, pp. 585–598, Feb. 2017.

[13] H. Bevrani and T. Hiyama, "On load-frequency regulation with time delays: Design and real-time implementation," *IEEE Trans. Energy Convers.*, vol. 24, no. 1, pp. 292–300, Mar. 2009.

[14] Y. Mi *et al.*, "Sliding mode load frequency control for multi-area time-delay power system with wind power integration," *IET Generat. Transm. Distrib.*, vol. 11, no. 18, pp. 4644–4653, 2017.

[15] C.-K. Zhang, L. Jiang, Q. H. Wu, Y. He, and M. Wu, "Delay-dependent robust load frequency control for time delay power systems," *IEEE Trans. Power Syst.*, vol. 28, no. 3, pp. 2192–2201, Aug. 2013.

[16] J. Li, Z. Chen, D. Cai, W. Zhen, and Q. Huang, "Delay-dependent stability control for power system with multiple time-delays," *IEEE Trans. Power Syst.*, vol. 31, no. 3, pp. 2316–2326, May 2016.

[17] Y. Tipsuwan and M.-Y. Chow, "Gain scheduler middleware: A methodology to enable existing controllers for networked control and teleoperation-part I: Networked control," *IEEE Trans. Ind. Electron.*, vol. 51, no. 6, pp. 1218–1227, Dec. 2004.

[18] S. Yan, Z. Gu, and S. K. Nguang, "Memory-event-triggered H_∞ output control of neural networks with mixed delays," *IEEE Trans. Neural Netw. Learn. Syst.*, early access, Jun. 4, 2021, doi: 10.1109/TNNLS.2021.3083898.

[19] C. Peng, Q.-L. Han, and D. Yue, "Communication-delay-distribution-dependent decentralized control for large-scale systems with IP-based communication networks," *IEEE Trans. Control Syst. Technol.*, vol. 21, no. 3, pp. 820–830, May 2013.

[20] H. Sun, C. Peng, D. Yue, Y. Wang, and T. Zhang, "Resilient load frequency control of cyber-physical power systems under QoS-dependent event-triggered communication," *IEEE Trans. Syst., Man, Cybern., Syst.*, vol. 51, no. 4, pp. 2113–2122, Apr. 2021.

[21] Y. Tang, D. Zhang, P. Shi, W. Zhang, and F. Qian, "Event-based formation control of multi-agent systems under DoS attacks," *IEEE Trans. Autom. Control*, vol. 66, no. 1, pp. 452–459, Jan. 2021.

[22] H.-T. Sun, C. Peng, and F. Ding, "Self-discipline predictive control of autonomous vehicles against denial of service attacks," *Asian J. Control*, Feb. 2022, doi: 10.1002/asjc.2749.

[23] F. Qu, E. Tian, and X. Zhao, "Chance-constrained H_∞ state estimation for recursive neural networks under deception attacks and energy constraints: The finite-horizon case," *IEEE Trans. Neural Netw. Learn. Syst.*, early access, Jan. 7, 2022, doi: 10.1109/TNNLS.2021.3137426.

[24] T.-Y. Zhang and D. Ye, "False data injection attacks with complete stealthiness in cyber-physical systems: A self-generated approach," *Automatica*, vol. 120, Oct. 2020, Art. no. 109117.

[25] S. Yan, Z. Gu, and J. H. Park, "Memory-event-triggered H_∞ load frequency control of multi-area power systems with cyber-attacks and communication delays," *IEEE Trans. Netw. Sci. Eng.*, vol. 8, no. 2, pp. 1571–1583, Apr.-Jun. 2021.

[26] J. Liu, Y. Gu, L. Zha, Y. Liu, and J. Cao, "Event-triggered H_∞ load frequency control for multiarea power systems under hybrid cyber attacks," *IEEE Trans. Syst., Man, Cybern., Syst.*, vol. 49, no. 8, pp. 1665–1678, Aug. 2019.

[27] X.-Z. Jin, W.-W. Che, Z.-G. Wu, and H. Wang, "Analog control circuit designs for a class of continuous-time adaptive fault-tolerant control systems," *IEEE Trans. Cybern.*, early access, Oct. 23, 2020, doi: 10.1109/TCYB.2020.3024913.

[28] X. Jin, S. Wang, J. Qin, W. X. Zheng, and Y. Kang, "Adaptive fault-tolerant consensus for a class of uncertain nonlinear second-order multi-agent systems with circuit implementation," *IEEE Trans. Circuits Syst. I, Reg. Papers*, vol. 65, no. 7, pp. 2243–2255, Jul. 2018.

[29] A. Seuret, F. Gouaisbaut, and Y. Ariba, "Complete quadratic Lyapunov functionals for distributed delay systems," *Automatica*, vol. 62, pp. 168–176, Dec. 2015.

[30] P. Kundur, *Power System Stability and Control*. 2nd ed. New York, NY, USA: Springer, 2014.

[31] S. Saxena and Y. V. Hote, "Load frequency control in power systems via internal model control scheme and model-order reduction," *IEEE Trans. Power Syst.*, vol. 28, no. 3, pp. 2749–2757, Aug. 2013.

[32] Y. C. Tian, D. Levy, M. O. Tade, T. Gu, and C. Fidge, "Queuing packets in communication networks for networked control systems," in *Proc. 6th World Congr. Intell. Control Automat.*, Dalian, China, vol. 1, 2006, pp. 205–209.

[33] Q. Feng and S. K. Nguang, "Stabilization of uncertain linear distributed delay systems with dissipativity constraints," *Syst. Control Lett.*, vol. 96, pp. 60–71, Oct. 2016.
[34] D. Rerkpreedapong, A. Hasanovic, and A. Feliachi, "Robust load frequency control using genetic algorithms and linear matrix inequalities," *IEEE Trans. Power Syst.*, vol. 18, no. 2, pp. 855–861, May 2003.
[35] C. A. R. Crusius and A. Trofino, "Sufficient LMI conditions for output feedback control problems," *IEEE Trans. Autom. Control*, vol. 44, no. 5, pp. 1053–1057, May 1999.

Shen Yan received the B.E. and Ph.D. degrees from the College of Electrical Engineering and Control Science of Nanjing Technology University, Nanjing, China. From 2017 to 2018, he was a visiting Ph.D. student with the University of Auckland, Auckland, New Zealand. From February 2022 to August 2022, he was a Visiting Scholar with Yeungnam University, Gyeongsan, South Korea. He is currently an Associate Professor with the College of Mechanical and Electronic Engineering, Nanjing Forestry University, Nanjing, China. His current research interests include networked control systems, event-triggered control, and their applications.

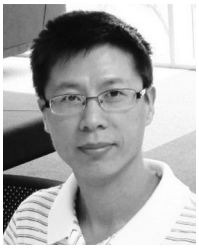

Zhou Gu (Member, IEEE) received the B.S. degree from North China Electric Power University, Beijing, China, in 1997, and the M.S. and Ph.D. degrees in control science and engineering from the Nanjing University of Aeronautics and Astronautics, Nanjing, China, in 2007 and 2010, respectively. From 1996 to 2013, he was with the School of Power engineering, Nanjing Normal University, as an Associate Professor. He was a Visiting Scholar with Central Queensland University, Rockhampton, QLD, Australia, and The University of Manchester, Manchester, U.K. He is currently a Professor with Nanjing Forestry University, Nanjing. His current research interests include networked control systems, time-delay systems, reliable control, and their applications.

Ju H. Park (Senior Member, IEEE) received the Ph.D. degree in electronics and electrical engineering from the Pohang University of Science and Technology (POSTECH), Pohang, South Korea, in 1997.

From May 1997 to February 2000, he was a Research Associate with Engineering Research Center-Automation Research Center, POSTECH. He joined Yeungnam University, Gyeongsan, South Korea, in March 2000, where he is currently the Chuma Chair Professor. He has coauthored the monographs *Recent Advances in Control and Filtering of Dynamic Systems with Constrained Signals* (New York, NY, USA: Springer-Nature, 2018) and *Dynamic Systems With Time Delays: Stability and Control* (New York, NY, USA: Springer-Nature, 2019) and is an Editor of an edited volume *Recent Advances in Control Problems of Dynamical Systems and Networks* (New York: Springer-Nature, 2020). His research interests include robust control and filtering, neural/complex networks, fuzzy systems, multiagent systems, and chaotic systems. He has published a number of articles in these areas. Since 2015, he has been a recipient of the Highly Cited Researchers Award by Clarivate Analytics (formerly, Thomson Reuters) and listed in three fields, Engineering, Computer Sciences, and Mathematics, in 2019, 2020, and 2021. He also serves as an Editor for the *International Journal of Control, Automation and Systems*. He is also a Subject Editor/Advisory Editor/Associate Editor/Editorial Board Member of several international journals, including *IET Control Theory & Applications, Applied Mathematics and Computation, Journal of The Franklin Institute, Nonlinear Dynamics, Engineering Reports, Cogent Engineering*, the IEEE TRANSACTION ON FUZZY SYSTEMS, the IEEE TRANSACTION ON NEURAL NETWORKS AND LEARNING SYSTEMS, and the IEEE TRANSACTION ON CYBERNETICS. He is a Fellow of the Korean Academy of Science and Technology (KAST).

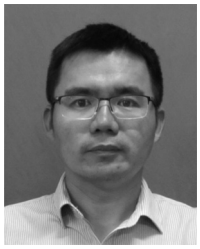

Xiangpeng Xie (Member, IEEE) received the B.S. and Ph.D. degrees in engineering from Northeastern University, Shenyang, China, in 2004 and 2010, respectively.

From 2010 to 2014, he was a Senior Engineer with Metallurgical Corporation of China Ltd., Beijing, China. He is currently a Professor with the Institute of Advanced Technology, Nanjing University of Posts and Telecommunications, Nanjing, China. His research interests include fuzzy modeling and control synthesis, state estimations, optimization in process industries, and intelligent optimization algorithms. He serves as an Associate Editor for the *International Journal of Control, Automation, and Systems* and the *International Journal of Fuzzy Systems*.

Chunxia Dou (Senior Member, IEEE) received the B.S. and M.S. degrees in automation from Northeast Heavy Machinery Institute, Qiqihaer, China, in 1989 and 1994, respectively, and the Ph.D. degree in electrical engineering from Yanshan University, Qinhuangdao, China, in 2005.

In 2010, she joined the Department of Engineering, Peking University, Beijing, China, where she was a Postdoctoral Fellow for two years. From 2005 to 2019, she was a Professor with the School of Electrical Engineering, Yanshan University. Since 2019, she has been a Professor with the Institute of Advanced Technology for Carbon Neutrality, Nanjing University of Posts and Telecommunications, Nanjing, China. Her current research interests include MAS-based control, event-triggered hybrid control, distributed coordinated control, multimode switching control, and their applications in power systems and smart grid.